

in Properties and Mechanisms of High T_c
Edited by Oguchi, Kawamura, and Sasakawa
North Hill
(1994)

Strongly Correlated Copper Oxide Layers: Insights From the Large N Expansion

Gabriel Kotliar

Serlin Physics Laboratory, Rutgers University Piscataway NJ 08854 USA

We report some results on generalized $SU(N)$ extended Hubbard and $t-J$ models, analyzed via the large N expansion technique, and discuss its possible relevance to the $N=2$ case of the copper oxide layers.

1. Introduction

In this talk I will report some results on generalized $SU(N)$ extended Hubbard^(1,2,3,4) and $t-J$ models,^(5,6) analyzed via the large N expansion technique. This method allows an essentially analytic solution of non-trivial models of strong correlation and gives insights into the possible behaviors of strongly interacting Fermi systems. One should keep mind, however, that some times the physics of $SU(N)$ models for N large differs considerably from the $SU(2)$ case. Comparison with exact numerical results and with experiments is therefore essential for assessing the applicability of the results of the large N theory to real materials. In the last year we have seen a significant improvement in the numerical techniques for systems with small but finite doping. The result of several of these calculations agree very well with the predictions of the large N theory, suggesting that once doping destroys the magnetic long range order the $\frac{1}{N}$ expansion is an asymptotic series down to $N=2$.

2. The extended Hubbard model

To motivate the large N approach I will start by listing some features of the CuO_2 layers which call for a theoretical treatment which is not perturbative in the parameters which appear in the hamiltonian:

a) The large on site copper repulsion nearly elements the configuration Cu^{++} . At half filling there is a 2 eV charge transfer gap. This upper Hubbard band feature persists upon doping. These facts indicate that correlations are still strong in the superconducting region of the

b) Strong covalency has been singled out as a unique feature of the CuO_2 system by many authors. That is the copper oxygen charge transfer energy $\epsilon_p - \epsilon_d$ is not too big. Evidence for that is the very rapid transfer of spectral weight from high to low energies upon doping observed in optical measurements.

c) The copper copper superexchange J is unusually large. In the heavy fermion systems, the heavy masses are the result of transferring the $\log 2$ entropy of each spin to the quasiparticle degrees of freedom at low temperatures. In the high- T_c systems the superexchange locks the spins. At temperatures less than J there is very little entropy left in the spin system and therefore there are no large mass renormalizations. This is an essential difference between the CuO_2 and the heavy fermion systems. Another possible manifestation of a strong superexchange is the opening of a spin gap above T_c in the lightly doped materials.

On the road to understanding the superconductivity in the CuO_2 system there are several theoretical questions that one would like to answer:

a) What is the nature of the single particle (hole) states created as one dopes a way from half filling.

b) What is the effective interactions between these single particle states. Resolution of these questions would lead to an effective low energy hamiltonian which can be used to describe the low energy transport dynamics in the normal state and to elucidate the origin and nature of the superconducting state.

These problems are hard for several reasons:

a) Doping is a singular perturbation, the excitation spectrum at finite doping is not analytically continuable from the excitation spectrum of the insulating compound.

b) In the region of interest $\frac{t_{pd}}{\epsilon_p^o - \epsilon_d^o}$ the ratio of the hybridization to the charge transfer energy is not really a small parameter.

c) In strongly correlated systems one has to build carefully the correct single particle excitations before attempting to compute their pairing interactions.

In a series of publications we have investigated this issue by studying different aspects of the following extended Hubbard model generalized to $SU(N)$. For an excellent review of work by other groups using the large N approach and more references see K. Levin et al.⁽⁷⁾

$$\begin{aligned}
H = & \epsilon_d^o \sum_{i\sigma} d_{i\sigma}^\dagger d_{i\sigma} + \epsilon_p^o \sum_{i\sigma\alpha=\pm y} p_{i\alpha\sigma}^\dagger p_{i\alpha\sigma} \\
& + i \sum_i \lambda_i (d_{i\sigma}^\dagger d_{i\sigma} + b_i^\dagger b_i - \frac{N}{2}) \\
& + \frac{V}{N} \sum_{i\sigma\sigma'\alpha=\pm z\pm y} d_{i\sigma}^\dagger d_{i\sigma'} p_{i\alpha\sigma'}^\dagger p_{i\alpha\sigma} \\
& - \frac{t_{pd}}{\sqrt{N}} \sum_{i\sigma} \{d_{i\sigma}^\dagger b_i (p_{i\sigma\sigma} - p_{i-z\sigma} + p_{i y\sigma} - p_{i-y\sigma} + c.c.) \\
& + \frac{t_{pp}}{N} \sum_{i\sigma} \{p_{i\sigma\sigma}^\dagger (P_{i y\sigma} - p_{i-y\sigma} + p_{i+z-y\sigma} - p_{i+z+y\sigma}) + c.c.\} \\
& + \frac{J}{N} \sum_{i i'} d_{i\sigma}^\dagger d_{i\sigma'} d_{j\sigma'}^\dagger d_{j\sigma} \quad (1)
\end{aligned}$$

The index σ runs from 1 to N . When $N = 2$ this hamiltonian reduces to the usual extended Hubbard model proposed by Emery⁽⁸⁾ and by Varma et al.⁽⁹⁾ as the minimal model to describe the essential physics of the CuO_2 layers. An explicit copper copper superexchange has been added to it so as to describe the physics of the superexchange to leading order in $\frac{1}{N}$.^(10,4)

This is only one possible generalization of the three band model to bring it to a $\frac{1}{N}$ framework. Other generalizations might be more suitable to describe other aspects of the physics. In particular $Sp(N)$ generalizations of $SU(2)$ give superconductivity in leading order in $\frac{1}{N}$ ⁽¹¹⁾ while other generalizations may be more suitable to describe finite temperature aspects of the onset of coherence problem.^(12,13,14)

The solution of the model proceeds by writing a path

integral representation of the model and decoupling various interaction terms by introducing suitable auxiliary fields. The functional integral at $N = \infty$ is dominated by a saddle point which describes Free Fermionic quasiparticles (QP) with strongly renormalized (quasiparticle level and quasiparticle dispersion) parameters. In calculating the response of the system to external fields the saddle point parameters change with the external fields giving rise to the different Fermi liquid renormalization which appear in the response functions.

The fluctuations of the bose field around the saddle point gives rise to residual interactions between the quasiparticles and generates the incoherent part of the one particle spectral weight.

At half filling this model displays a metal insulator transition as a function of $\frac{t_{pd}}{\epsilon_p^o - \epsilon_d^o}$. We will assume that $\epsilon_p^o - \epsilon_d^o$ is sufficiently large to be on the insulating side of the transition. At half filling, when $t_{pp} = 0$ the one particle spectral function has two broad features, (of width $\frac{t_{pd}^o}{\epsilon_p^o - \epsilon_d^o}$) around the bare levels $\epsilon_p^o - \epsilon_d^o$. In the ionic limit they correspond to the Cu^{++} to Cu^+ and O^{--} to O^- transitions respectively. It was shown in ref. c) that upon doping new quasiparticle states are introduced in the charge transfer gap, within $\frac{t_{pd}^o}{\epsilon_p^o - \epsilon_d^o}$ of ϵ_p^o for hole doping. This is illustrated schematically in Fig. 1.

This states form a narrow band around the renormalized level ϵ_d . This states have a Luttinger fermi surface containing $1 + \delta$ holes, and constitute the dispersive features observed in angle resolved photoemission. It is important to emphasize that the chemical potential has a discontinuity, $\Delta\mu$ when δ crosses zero and we go from electron to hole doping. This discontinuity gets smaller as we decrease $\epsilon_p^o - \epsilon_d^o$ and approach the metal insulator transition. At this point the charge transfer gap vanishes. Since the charge transfer gap is finite at half filling it is not possible within this framework to account for the pinning of the chemical potential observed in some photoemission experiments. We find that the chemical potential moves to the renormalized d level which sits at the bottom of the upper Hubbard Band in complete analogy with the phenomenology of Mott Hubbard Systems.

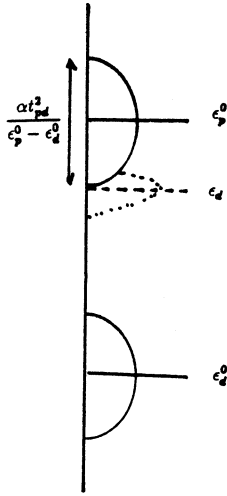


FIGURE 1

One particle density of states (schematically) at zero (full line) and modification of the spectral function upon doping (dotted line). ϵ_d is the renormalized quasiparticle level.

Having established the nature of the single particle excitations we turn now to their effective interactions. The Gaussian fluctuation of the bose fields around their saddle point values describe the residual interactions between the quasiparticles. They are represented diagrammatically in Fig. 2.



FIGURE 2

Figure 2: Effective interaction to leading order in $\frac{1}{N}$. Dashed lines are bare bose propagations. External lines are in the lowest band. Internal bubbles are of type 11, 12 and 13.

There are three kinds of polarization bubbles 11, 12, 13 which correspond to intraband transitions in the lower

quasiparticle band and virtual polarization processes via unoccupied bands 2 and 3 respectively.

If we neglect the 12 and 13 processes the effective interactions between the quasiparticles in the lowest band are those of the $t-J$ model generalized to $SU(N)$. While the RPA sum in Fig. 2 resembles an attractive interaction mediated by a single boson exchange, this impression is misleading. The slave boson interaction is repulsive. It is composed of a repulsive pseudopotential among the quasiparticles which reflects the original infinite on site repulsion between the particles and (if the exchange J is present) a residual spin exchange interaction between the quasiparticles which reflects the original superexchange among the copper spins. This superexchange gives rise to a very weak attraction in the d wave channel.

When we study the $t-J$ model, we therefore neglect the interband processes and a natural question is when do they have a qualitatively new effect?

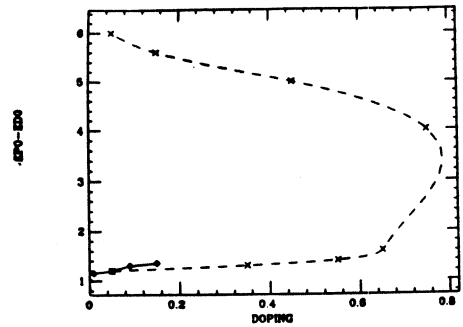


FIGURE 3

Phase diagram of the extended Hubbard model for $V=2.5$ and $t_{pp} = 0$. The dashed line indicates the locus of points where the compressibility diverges. The straight line is the valence instability line. Surrounding the dashed lines there is a region of phase separation.(not indicated in the figure).

We have followed the suggestion of Varma et al.⁽⁹⁾ and studied the effect of a copper oxygen repulsion V of the order of t_{pd} . We have found⁽³⁾ that V enhances the

attraction produced by the 12 and 13 processes over the repulsive component arising for the 11 processes. When $\epsilon_p^o - \epsilon_d^o$ is of the order of tpd , i.e. not too far from the metal charge transfer insulator transition, we find that a V of order tpd tips the balance between attractive and repulsive forces and gives rise to a net attractive interaction between the quasiparticles. This attraction gives rise to a region of phase separation which surrounds the region of negative compressibility shown in fig. 3 and 4. Notice that the details of the phase separation region depend on microscopic parameters like the strength of tpd ,⁽¹⁶⁾ but the existence of phase separation is a generic feature of a large copper oxygen repulsion. Outside, but near the region of phase separation we found that the effective interactions between the quasiparticles are attractive in the s wave channel.

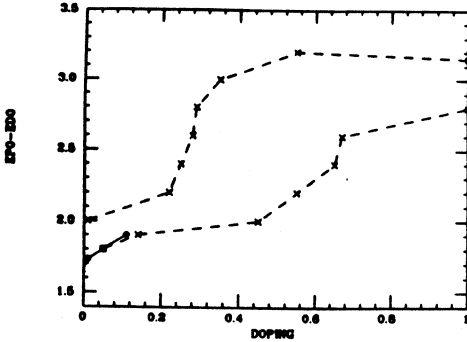


FIGURE 4

Phase diagram of the extended Hubbard model for $V=2.3$ and $t_{pp} = .2$. The dashed line indicates the locus of points where the compressibility diverges. The straight line is the valence instability line. Surrounding the dashed lines there is a region of phase separation. (not indicated in the figure).

The origin of this attraction can be understood in simple physical terms. The term V tries to make $n_p n_d$ close to zero, by making either $n_p \sim 1$ or $n_d \sim 0$ or $n_d \sim 1$ and $n_p \sim 0$. The hybridization tpd opposes this effect. Mathematically $V \gg tpd$ gives rise to multiple solutions of the mean field equations which deter-

mine the quasiparticle level. Physically, this indicates the possible coexistence of different valences. When a fluctuation from copper to oxygen takes place the term $V n_p n_d$ becomes ineffective and it becomes energetically advantageous to add a second oxygen near by, this is the origin of the attractive interaction.

A calculation is needed to establish that this attractive component of the interaction can actually dominate over the other repulsive interactions which are always present and to determine that the attraction gives rise to s wave superconductivity and not to a CDW or a phase separated state.^(17,18,19) In the large N limit, for infinite copper on site repulsion in ref (5).

The scenario linking the copper oxygen repulsion, multiple (valences) solution of the mean field equations phase separation and s wave superconductivity occurs also in a weak coupling Hartree Fock analysis. We present it here because it brings very clearly the generic features of the connection between valence instabilities, superconductivity and phase separation and clarifies the specific effects which originate from a very large copper copper repulsion and the proximity to the metal charge transfer insulator point.

The Hartree Fock equations for the renormalized p and d levels are formally identically to the equations for the spontaneous magnetization in the classical Ising model. $\langle n_d \rangle - \langle n_p \rangle$ plays the role of magnetization while $\epsilon_p^o - \epsilon_d^o - (\frac{U}{4} - \frac{U_p}{8})(1 + \delta)$ plays the role of external magnetic field (U_p is the oxygen oxygen repulsion). In our problem tpd and $(V - \frac{U}{8} - \frac{U_p}{16})$ play the role of the Ising model temperature and magnetic exchange respectively. The renormalized copper oxygen level difference $\epsilon_p - \epsilon_d$ is analogous to the internal (Weiss) field in the Ising model.

When the coupling J is above a critical value (i.e. for $V > V_c$) there are two possible values of the magnetization. When one moves across the critical line by applying a field (i.e. moving $\epsilon_p^o - \epsilon_d^o$) the magnetization (i.e. the valence) jumps. We call this line the valence instability (VI) line and it is shown by the dotted line in fig. 3. This line ends in a second order valence instability point, denoted by X . Since at that line two different mean field solutions cross as a function of doping it is

clear that the total energy as a function of doping has the wrong convexity, i.e. there is a region of phase separation surrounding the VI line. As one reduces $\epsilon_p^o - \epsilon_d^o$ approaching the VI point, the discontinuity disappears but the negative compressibility remains. We draw with a dash dotted line the line where the compressibility diverges. This is the charge transfer instability CTI line. It is important to emphasize that for moderate values of U_{dd} the charge transfer instability line (i.e. the line where $(\frac{\partial n_p - n_d}{\partial \mu})_{\epsilon_p^o - \epsilon_d^o}$ diverges, coincides with the line where the compressibility $(\frac{\partial n}{\partial \mu})_{\epsilon_p^o - \epsilon_d^o}$ diverges. The zero sound mode becomes unstable at that line while the charge transfer excitation does not soften much at the CTI. Because of the occurrence of phase separation $\epsilon_p - \epsilon_d$ cannot be adjusted to zero, when V is sufficiently large.

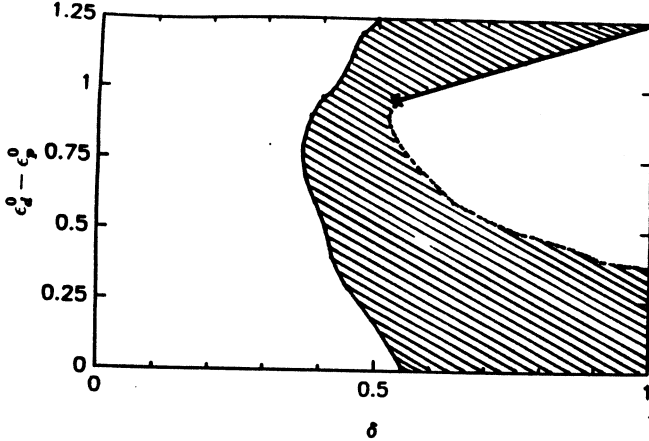


FIGURE 5

Phase diagram for $U = 3, V = 2.5$, and $U_p = 1$. The solid line is a line of the first order transition ending in a VI critical point, "x". ϵ changes discontinuously across this line. The dashed line is a locus of the points where the compressibility diverges. The hatched area is obtained by Maxwell construction.

The analogy between the weak coupling and the strong coupling scenarios as displayed in figs. 3-5 is now clear. The main difference between the small U_{dd} and the $U_{dd} = \infty$ limit is the region of parameters where phase separation occurs. This is related to the different depen-

dence of the kinetic energy on doping, for $U_{dd} = \infty$ the kinetic energy decreases as δ is reduced and phase separation is encountered when the doping is decreased. For small U_{dd} the kinetic energy decreases when the doping increases and phase separation occurs upon increasing doping. Some features of our analysis have appeared in earlier exact diagonalization studies in small clusters. It would be interesting to determine the phase diagram for intermediate values of U by quantum monte carlo calculation to establish whether the $U_{dd} = \infty$ or the small U_{dd} picture is more appropriate for realistic parameters of the Hamiltonian of the copper oxide layers.

3. The SU(N) t-J model

In the second part of this talk I would like to report on some progress in understanding the physics of the t-J model at moderate doping using the large N technique.^(5,6) The t-J model with SU(2) generalized to SU(N) is defined by the following model hamiltonian.⁽⁶⁾

$$\begin{aligned}
 H = & \frac{-t}{N} \sum_{ij} b_i f_{\sigma i}^+ b_j^+ f_{\sigma j} - \mu \sum_{\sigma} f_{\sigma i}^+ f_{\sigma i} \\
 & + \frac{J}{N} \sum_{ij} f_{i\sigma}^+ f_{i\sigma'} f_{j\sigma'}^+ f_{j\sigma} \\
 & + i \sum_i \lambda_i (b_i^+ b_i + \sum_{\sigma} f_{i\sigma}^+ f_{i\sigma} - \frac{N}{2}) \quad (2)
 \end{aligned}$$

σ is an index which runs from 1 to N. μ is the chemical potential adjusted to have δ holes, i. e. $\sum_{\sigma} \langle f_{\sigma i}^+ f_{\sigma i} \rangle = \frac{N}{2}(1 - \delta)$. In the following ij will run over a square lattice nearest neighbors. The motivation for this investigation is manifold. Anderson⁽²⁰⁾ has suggested that the t-J model is the minimal hamiltonian which captures the essential physics of the CuO_2 planes. We have seen that for $\epsilon_p^o - \epsilon_d^o$ sufficiently large and small V the generalized SU(N) three band extended Hubbard model gives the same low energy hamiltonian as the generalized SU(N) t-J model, when N is large. Finally, the t-J model is the simplest model capturing the physics of strong correlation and magnetic exchange. There is now a substantial number of exact results^(21, 22) in small clusters and they give us an indication of when the predictions of the large N expansion can be safely extrapolated to $N=2$.

The $N = \infty$ phase diagram is shown in fig. 6, at large dopings or for small values of $\frac{J}{t}$ there is a Fermi liquid phase where the band order parameter $\Delta = J < f_i^\dagger f_j >$ is uniform in space. This phase describes a strongly (antiferromagnetically) correlated Fermi liquid. Exactly at $\delta = 0$ the ground state is a fully dimerized insulating phase. The nature of the ground state at very small doping on large $\frac{J}{t}$ has not been fully elucidated. There are tendencies towards dimerization and flux condensation but the optimal flux patterns remains to be found. In the case where of nearest neighbor hopping on the square lattice we have argued⁽²⁵⁾ that these details are irrelevant since at small doping the system phase separates between a uniform (fermi liquid) phase (with a large concentration of holes) and an insulating dimer phase. the phase separation line is shown in fig (6).

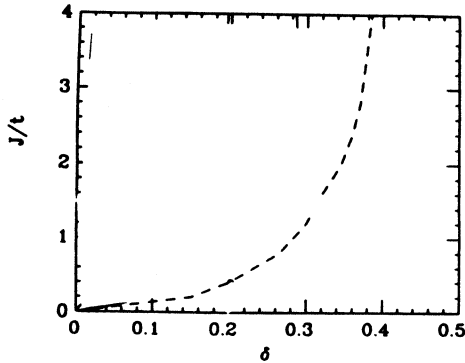


FIGURE 6

Phase diagram of the $t - J$ model with nearest neighbor hopping and exchange. The dashed line is the phase separation line.

The uniform phase is stable, because the Fermi liquid state can gain a substantial fraction of the magnetic energy⁽⁶⁾ while simultaneously minimizing the kinetic energy. We now turn to its physical properties.

The one particle Green's function is given by:

$$G_{ij}(\tau) = - \langle T(f_i(\tau)b_i^\dagger(\tau)b_j(o)f_j^\dagger(o) \rangle \quad (3)$$

The Fourier transform of the retarded Green func-

tion is expressed in terms of 3 self energies as

$$G_R(K, \omega) = \frac{\langle b \rangle + \Sigma_{on}(K, \omega)^2}{\omega - \epsilon_K - \Sigma_n(K, \omega)} + \Sigma_{inc}(K, \omega) \quad (4)$$

Z. Wang, Y. Bang and I⁽⁶⁾ have evaluated (eq. 5) to next to leading order in $\frac{1}{N}$. The corresponding spectral function is plotted for several wave vectors in fig. 7. The $N = \infty$ contributions give rise to the main dispersive features while the $\frac{1}{N}$ corrections generate a broad incoherent background.

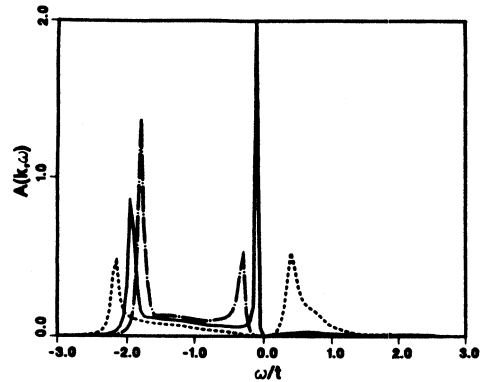


FIGURE 7

Spectral function for $J/t = .36 = .2$ at $k = .86(\frac{\pi}{2}, \frac{\pi}{2})$ solid $k = .67(\frac{\pi}{2}, \frac{\pi}{2})$ chain dot and $k = 1.2(\frac{\pi}{2}, \frac{\pi}{2})$ dashed line.

To understand the numerical results its useful to summarize some features of the collective modes of this model.⁽⁶⁾ There is a density fluctuation mode ω_q , which for small doping, disperses as

$$\omega_q \sim -t(\cos q_x + \cos q_y - 2) \quad (5)$$

over most of the zone while reduces to the usual zero sound mode at long wavelengths. This is precisely the dispersion of the slave boson, so we find that even if the phase of the slave boson does not have physical meaning its magnitude can be identified with a field that describes

the propagation of a bare hole in a $U = \infty$ system. It may correspond to Anderson's concept of a holon.⁽²⁷⁾ There are also spin singlet modes which describe chiral fluctuations^(28,29) of the spin system which generate fluctuating electric currents. When N is large we find that long wavelength chiral fluctuations are energetically very costly. There are however very low lying fluctuations with wave vector near (π, π) . We note that recent numerical studies⁽²²⁾ also show a large enhancement of the staggered flux relative to the uniform flux fluctuations when $N = 2$. The sharp peaks in the spectral function correspond to quasiparticle states with dispersion⁽⁵⁾

$$E_{\mathbf{K}} = -(2\Delta + \delta t)(\cos K_x + \cos K_y) + (\mu + \lambda_o) \quad (6)$$

Δ is the bond order parameter of the order of J . $-\mu + \lambda_o$ is an offset which allows to satisfy Luttinger's theorem. The Fermi surface to leading order in $\frac{1}{N}$ is unrenormalized and its volume contains $1 - \delta$ states. Notice that the $N = \infty$ quasiparticle mass is proportional to $\frac{1}{(6t+2\Delta)}$. Since $\Delta \sim J$ remains finite as the doping approaches zero the specific heat and the susceptibility are finite and scale as $\frac{1}{J}$ for low doping.

Here we see explicitly how the non-perturbative introduction of the magnetic superexchange eliminates the heavy masses characteristic of the heavy fermion systems. The finite quasiparticle mass should be contrasted with the optical mass defined by the integrated strength of the low frequency optical absorption which scales when $N = \infty$ as $\frac{1}{6t}$. This is because the magnetic effects which give a finite quasiparticle mass at half filling cancel out completely in the transport of charge.

The $N = \infty$ limit of the $t - J$ model illustrates in a solvable model how a strongly correlated system can have a large Luttinger Fermi surface, a quasiparticle mass which scales as $\frac{1}{J}$, and a plasma frequency squared proportional to the number of holes.⁽¹⁾ The width of the peaks in the spectral function is related to the imaginary part of the normal self energy Σ_n . We found⁽²⁾ that $Im\Sigma_n \sim \frac{\omega^2}{\omega_c}$ for $\omega < \omega_c$ and $Im\Sigma_n \sim \omega$ for $\omega > \omega_c$.

For N large ω_c is a small fraction of J . It is the characteristic scale of incommensurate flux fluctuations. Its vanishing signals the onset of a flux density wave

instability.⁽³²⁾ Non Gaussian fluctuations, which become important for small N , reduce the scale ω_c even further. The bulk of the incoherent part of the spectral weight can be understood in terms of the convolution of the quasiparticle and the "holon" spectral weight which appears in the three self energies Σ_n , Σ_a and Σ_{inc} . The three self energies give comparable contributions to the spectral weight. However Σ_a contributes negative spectral weight at positive frequencies and cancels the contributions of Σ_{inc} and Σ_n at $\omega > 0$ almost completely.

This cancellation is another manifestation of the $U = \infty$ constraint which makes it much easier to remove a particle than to add one close to half filling.

The total spectral density (integrated over the wave vector) which is measured in tunnelling is given by:

$$-\frac{1}{\pi} \Sigma_k Im G_R(\omega, k) \sim [\delta + \frac{|\omega|}{t} \theta(-\omega)] \quad (7)$$

The deviations from particle-hole symmetry are rather small, i.e., $\theta(\frac{|\omega|}{t})$. It is interesting to compare this result with the large ($\simeq \frac{J}{t}$) asymmetry in the phase where the slave bosons are not condensed.⁽²⁹⁾

The large N expansion does not describe the behavior of the $N = 2$ model at half filling because a phase transition as a function of N between a dimerized and an antiferromagnetic Neel phase takes place at $N = 4$.⁽³¹⁾ It is important to emphasize that our results are consistent with exact small cluster diagonalization studies by Stephan and Horsch,⁽²²⁾ suggesting that for moderate dopings, once the magnetic long range order is destroyed, the $\frac{1}{N}$ expansion gives a good account of the ground state properties of the $t - J$ model.

Finally, I would like to discuss briefly the behavior of the model for small dopings, i.e. once the uniform phase is destabilized. We have already alluded to the simplest possible scenario i.e., phase separation between a dimerized insulator and a Fermi liquid metal. More complicated scenarios are possible. A finite next nearest neighbor hopping t' of order J stabilizes the staggered flux phase (SPP) against phase separation.⁽³²⁾ Z. Wang, X. Wang and I have studied the thermodynamics and transport properties of the staggered flux phase⁽³²⁾ to leading order in $\frac{1}{N}$. The behavior we found with $t = .45$

and $t' = J = .13$ is very reminiscent of the physical properties of the $La_{2-x}Sr_xCuO_2$ system.⁽³⁴⁾ The magnetic susceptibility χ as a function of doping has a maximum at a value $\delta_m \sim .25$. For $\delta < \delta_m$ χ increases with temperature, a result of the opening of a spin pseudo-gap by the staggered flux condensation. For larger dopings, χ decreases with temperature since the staggered flux pattern disappears and the SPP crosses over to the uniform phase. The Hall number, n_H , increases with doping, and for small doping n_H increases with temperature. Other observable properties of the SPP have been discussed recently by Hsu et. al. These results, at very small dopings, should only be taken as very qualitative indications of what can happen at $N=2$. We know that the next order in $\frac{1}{N}$ introduces small incommensurate modulations of the flux pattern and a pairing interaction in the s wave channel.

4. Conclusion

In conclusion we showed how one can generate a $\frac{1}{N}$ expansion for the extended Hubbard model. This expansion is not based on the smallness of any parameters in the Hamiltonian and displays non-perturbative effects like the formation of quasiparticles in the charge transfer gap upon doping, and a metal charge transfer insulator transition as $\epsilon_p^0 - \epsilon_d^0$ is reduced.

A similar expansion was carried out for a generalized $t-J$ model. Comparing these expansions we established the regime of parameters in which the extended Hubbard model and the $t-J$ model generate equivalent low energy hamiltonians. We also established the regime of parameters in which the finiteness of $\epsilon_p^0 - \epsilon_d^0$ gives rise to qualitatively new effects, and extended the ideas of Varma et al. to the large U_{dd} limit. A particularly simple picture of the attraction generated by the copper oxygen repulsion valid for strong and weak coupling emerged from this treatment.

The same large N technique was used to analyze the $t-J$ model at moderate doping levels. The large N expansion provides the concepts to understand the complex behavior of the spectral function and the response functions of this strongly correlated Fermi system.

The good agreement between the large N calculations and the small cluster exact diagonalization results is at this point very encouraging.

Acknowledgment

This research was supported by the NSF under grant DMR 89-15895.

References

1. G. Kotliar, P. A. Lee and N. Read, Physica C 153-155, 538 (1988).
2. M. Grilli, G. Kotliar and A. Millis, Phys. Rev. B 42, 329 (1990).
3. M Grilli, R. Raimondi, C. Castellani, C. Dicastro and G. Kotliar, Phys. Rev. Lett. 67, 259 (1991).
4. G. Castellani, M. Grilli and G. Kotliar, Phys. Rev. B 43, 8000 (1991).
5. M. Grilli and G. Kotliar, Phys. Rev. Lett. 64, 1170.
6. Z. Wang, Y. Bang and G. Kotliar, RU preprint.
7. K. Levin and Q. Si, Physica C 174 460 (1991).
8. V. J. Emery, Phys. Rev. Lett. 58, 2794 (1987).
9. C. Varma, S. Schmitt-Rink and E. Abrahams, Solid State Commun. 62, 681 (1987).
10. G. Kotliar, Int. Jour. of Mod. Phys. B, 1, 711 (1988).
11. N. Read and S. Sachdev, Phys. Rev. Lett. 66, 1773 (1991).
12. D. Doucot and J. Rodriguez, Europhys. Letters 11, 451 1990.
13. G. Kotliar, International Journal of Modern Physics B Vol. 5, Nos. 1 & 2 (1991) 341-352.
14. Y Oono T Matsuura and Y Kuroda J Phys. Soc. Jpn 57, 1687 (1988) .
15. M. Grilli, R. Raimondi, C. Castellani, C. Dicastro, G. Kotliar, Int. Jour. Mod. Phys. 5, 309 (1991).

16. Y. Bang, C. Castellani, C. Dicastro, M. Grilli, G. Kotliar, and R. Raimondi, to be published.
17. S. A. Trugman, *Physica Scripta*. Vol. T27, 113 (1989).
18. J. E. Hirsch, E. Loh, Jr., D. J. Scalapino, and S. Tang, *Phys. Rev. B* 39, 243 (1989).
19. Y. Bang, G. Kotliar, M. Grilli, R. Raimondi, C. Castellani, *Phys. Rev. B* 43, 13724 (1991).
20. P. W. Anderson, *Science* 235, 1196 (1987).
21. W. Stephan and P. Horsch, *Phys. Rev. Lett.* 66, 2258 (1991).
22. D. Poilblanc, E. Dagotto and J. Riera, *Phys. Rev. B* 7899 (1991).
23. T. Dombre and G. B. Kotliar, *Phys. Rev. B* 39, 855 (1989).
24. J. Brad Marston and I. Affleck, *Phys. Rev. B* 39, 11538 (1989).
25. M. Grilli, C. Castellani and G. Kotliar, preprint.
26. D. Morse and T. Lubensky, *Phys. Rev. B* 43, 10436 (1991). S. Sachdev *Phys. Rev. B* 41, 4502 (1990)
27. P. W. Anderson, *Physics Reports* 184, 195 (1989).
28. X. Wen, F. Wilckek and A. Zee, *Phys. Rev. B* 39, 11413 (1989).
29. N. Nagaosa and P. Lee, *Phys. Rev. Lett.* 64, 1170 (1990).
30. Z. Wang, G. Kotliar, and X. Wang, *Phys. Rev. B* 42, 8670 (1990).
31. J. B. Marston, *Phys. Rev. Lett.* 64, 1166 (1990).
32. Z. Wang, X. Wang and G. Kotliar, RU preprint.
33. T. Hsu, B. Marston and I. Affleck, *Phys. Rev. B* 43, 2866 (1991).
34. S. Uchida et al., *Phys. Rev. B* 43, 7942 (1991). M. Takagi et al., *Phys. Rev. B* 40, 2254 (1989). M. Suzuki, *Phys. Rev. B* 39, 2312 (1989).